

Original article

DOI: <https://doi.org/10.18721/JPM.15207>

ANALYSING THE EFFECT OF A CRANIUM THICKNESS ON A BRAGG PEAK RANGE IN THE PROTON THERAPY: A TRIM AND GEANT4 BASED STUDY

F. Ekinçi ¹✉, E. Bostancı ², M. S. Güzel ², Ö. Dağlı ¹

¹ Gazi University, Ankara, Turkey,

² Ankara University, Ankara, Turkey

✉ fatih.ekinci2@gazi.edu.tr

Abstract. Cancer treatment with proton therapy, starting in 1946, continues with the treatment of 200,000 patients worldwide as of 2020. The energy release of protons in tissue and tissue equivalent (water) material is shown by Bragg curves. The main reason why proton beams are preferred in radiotherapy is that the proton beams continue on their way by giving maximum energy to the tissue to be treated and giving the least damage to the healthy tissue. In this study, with the help of Monte Carlo-based GEANT4 and TRIM simulation programs, Bragg peak positions in the 60 – 130 MeV energy range are given for water and brain by using the relativistic Bethe – Bloch equation. The difference between GEANT4 and TRIM was 7.4 % on average in the water phantom, while the difference was 7.6 % in the brain phantom. Bragg peak position was calculated for water and brain phantoms at 0.6, 0.8 and 1.0 cm thicknesses, which is suitable for the average thickness of the cortical bone in the skull. An average of 8.1 and 7.8 % deviations were detected between the two simulation systems in the cortical bony, water and brain phantoms with three different thicknesses. The values found were compared with the clinical studies available in the literature.

Keywords: Monte Carlo, GEANT4, TRIM, radiation therapy, proton therapy, LET

Citation: Ekinçi F., Bostancı E., Güzel M. S., Dağlı Ö., Analysing the effect of a cranium thickness on a Bragg peak range in the proton therapy: a TRIM and GEANT4 based study, St. Petersburg State Polytechnical University Journal. Physics and Mathematics. 15 (2) (2022) 64–78. DOI: <https://doi.org/10.18721/JPM.15207>

This is an open access article under the CC BY-NC 4.0 license (<https://creativecommons.org/licenses/by-nc/4.0/>)



Научная статья

УДК 615.849.12

DOI: <https://doi.org/10.18721/JPM.15207>

АНАЛИЗ ВЛИЯНИЯ ТОЛЩИНЫ ТКАНЕЙ ЧЕЛОВЕЧЕСКОГО ЧЕРЕПА НА ДИАПАЗОН ПИКОВ БРЭГГА ПРИ ПРОТОННОЙ ТЕРАПИИ С ПОМОЩЬЮ ПРОГРАММ TRIM И GEANT4

Ф. Экинджи ¹✉, Э. Бостанджи ², М. С. Гузель ², О. Дагли ¹

¹ Университет Гази, г. Анкара, Турция;

² Университет Анкары, г. Анкара, Турция

✉ fatih.ekinci2@gazi.edu.tr

Аннотация. Лечение рака с помощью протонной терапии, начатое в 1946 году, продолжает развиваться по всему миру, и, например, в 2020 г. этот метод применяли у 200 тыс. пациентов. Энерговыведение протонов в человеческой ткани и тканевом эквиваленте (воде) контролируется кривыми Брэгга. Преимущество протонных лучей заключается в том, что они отдают максимальную энергию обрабатываемой ткани, проникая вглубь, и при этом наносят минимальный ущерб здоровым тканям. В данном исследовании представлены позиции пиков Брэгга в диапазоне энергий 60 – 130 МэВ для воды и мозга, полученные с помощью уравнения Бете – Блоха и программ моделирования GEANT4 и TRIM (основаны на методе Монте-Карло). Сравнение результатов, полученных через GEANT4 и TRIM, показало разницу в среднем 7,4 % для водного фантома и 7,6 % для мозгового. Положения пиков Брэгга были рассчитаны для фантомов воды и мозга при значениях толщины тканей 0,6, 0,8 и 1,0 см, что соответствует средней толщине коркового слоя черепной кости. Значения отклонений между двумя системами моделирования, составили в среднем 8,1 и 7,8 % для двух фантомов (три значения толщины тканей). Полученные в работе расчетные значения были сопоставлены с данными опубликованных клинических исследований.

Ключевые слова: метод Монте-Карло, GEANT4, TRIM, лучевая терапия, протонная терапия, LET

Для цитирования: Экинджи Ф., Бостанджи Э., Гузель М. С., Дагли О. Анализ влияния толщины тканей человеческого черепа на диапазон пиков Брэгга при протонной терапии с помощью программ TRIM и GEANT4 // Научно-технические ведомости СПбГПУ. Физико-математические науки. 2022. Т. 15. № 2. С. 64–78. DOI: <https://doi.org/10.18721/JPM.15207>

Статья открытого доступа, распространяемая по лицензии CC BY-NC 4.0 (<https://creativecommons.org/licenses/by-nc/4.0/>)

Introduction

Heavy ion beams have been the focus of radiation oncology for over 60 years due to their superior physical and biological properties compared to conventional high-energy photon beams [1]. Protons are currently used in more than 61 facilities worldwide [2], there are 16 centers in clinical operation in Europe, and many centers are under construction [3]. A single energy heavy ion beam releases most of its energy in a narrow depth range known as the Bragg peak, with the peak dose depth determined by the ion species and target properties [4]. Due to the narrow depth range of the Bragg peak, minimal lateral scattering [5, 6] combined with the high relative biological activity of heavy ions, heavy ion therapy provides a therapeutic dose that is well suited for the target volume, with an input dose much lower than it is possible with photon therapy [7]. Heavy-ion beams minimize damage to adjacent healthy tissues, which is particularly useful for treating deeply located tumors [4, 7]. However, due to large dose gradients, deviations between the treatment plan and the delivered dose distribution can have serious adverse effects on healthy tissue, especially if the treatment site is close to the organ at risk. Accurate, real-time measurement of dose distribution during irradiation minimizes errors between the treatment plan and the actual delivered dose [7]. The success of heavy ion therapy depends on accurate dose measurement and dosimetric accuracy obtained with the help of semi-analytical pencil beam algorithms [8].

Regarding the accuracy in dose measurement, general purpose Monte Carlo (MC) codes are considered the "gold standard" [9]. Different MC simulation codes are used in proton therapy centers to improve dose estimations over standard methods using analytical or semi-empirical dose algorithms [10 – 14]. Potentially adopting systematic and user-friendly use of general-purpose MC tools for quality assurance (QA) and research requires reliable as well as generally applicable interfaces for connecting MC tools and incorporating them into the radiation oncology workflow [15]. GEANT4 and TRIM MC simulation codes are used in proton therapy applications to compare energy distributions in simple water phantoms, phantoms with complex structures, and phantoms with voxelized geometry based on clinical CT data [16]. An advantage of using Geant4 and TRIM is that both are based on the MC method, which can yield the secondary knock-on atom (SKA) energy spectrum of a composite material or alloy, whereas the analytical INtegrated model for Competitiveness Assessment of SMRs (INCAS) code only describes cascades in pure metal [17]. Another advantage is that Geant4 and TRIM provide the spatial distribution of displacements [20]. In other words, the effect of neutron spectrum and dispersion or material shape on the distributions of defects and production rates can be simulated using this method [17].

In this study, the Bragg curves formed by the proton beam in both a homogeneous water phantom and a heterogeneous one such as the brain were confirmed by experimental and computational studies in the literature with the help of frequently used GEANT4 and TRIM MC simulation systems. The behavior of the therapeutic proton beam was found with the help of two simulation systems in the presence of 0.6, 0.8 and 1.0 cm thick cortical bone placed in front of both the water phantom and brain one. All the data from the two simulation systems were compared.

Materials and methods

Monte Carlo (MC) codes are a simulation technique developed for highly accurate solutions of analytically complex problems in dose measurements [9]. So the MC is capable of following and calculating all interactions of particles within the target [18]. One of these simulation systems is the TRIM (TRANsport of Ions in Matter) simulation program. Parameters such as the type of targeted particle beam, the particle number, energy, the structural and geometric properties of the target, the angle of incidence of the particle beam at the target and the probability number can be entered from the TRIM screen. TRIM saves and displays all calculation fields. TRIM calculates and tabulates all kinetic events related to the interaction processes of ions with the target, such as damage, scattering, ionization, phonon production and recoil [19]. The displacement of the target atoms caused by the collision cascades and the cavities occurring in the target crystal structure are calculated in detail. The number of displacement collisions of the target atoms indicates how many target atoms are activated at energies above the displacement energy. The spaces left behind when the recoil atom leaves its original region are called target spaces. A vacuum does not occur unless a moving atom hits the target's stationary atom and transfers enough energy to displace it [19, 20]. The "Detailed Calculation with Full Damage Cascades" type option was selected in the calculations from the display window of the TRIM program. The particle number of the heavy ion

beam was entered as 106 particles in the “Total Number of Ions” tab. Calculation outputs were declared in the "Output disk files" tab, and the ion range, recoils, sputtered atoms and collision details output files were selected. The phantom type was created in the "Compound Dictionary" tab and its geometry was created in the "Add New Layer" section.

The GEANT4 (GEometry ANd Tracking, version 4) is an MC-based simulation program, capable of simulating all interactions of the ions passing through the material in the target. GEANT4 consists of two user classes, “Mandatory Classes” and “Action Classes”, in simulation software [21]. In this study, mandatory classes G4V User Detector Construction, G4V User Primary Generator Action and G4V User Physics List were used. As for the action classes, G4 User Run Action, G4 User Event Action, G4 User Stacking Action, G4 User Tracking Action and G4 User Stepping Action classes were used. The simulation detector is designed as a cube-shaped ion chamber with an edge length of 1 cm and quenching gas Ar. The step range (Range cut) was taken as 0.01 cm.

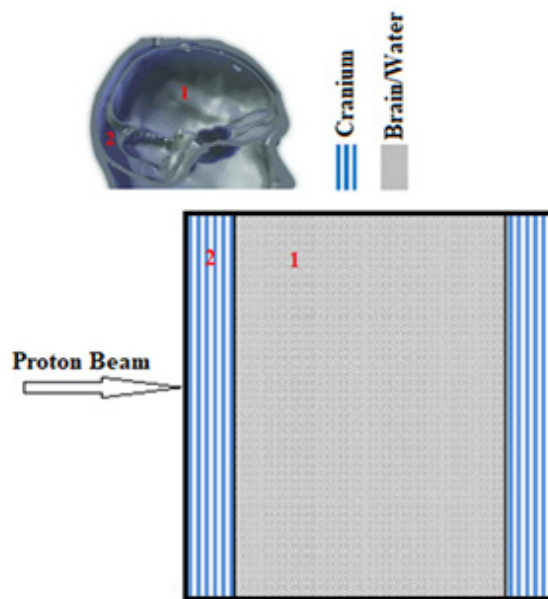


Fig. 1. The phantom cross-section geometry:
 1 – water or brain, 2 – cranium; section 2 is removed only for brain and water measurements

Table 1

The main information about biomaterials used in the cross-section phantom [25, 26]

Biomaterial	Atomic percentage, %	Atomic density, 10^{22} atom/cm ³	Density, g/cm ³
Cranium	H 3.4; O 43.5; C 15.5; N 4.2; S 0,3; Ca 22.5; P 10.3; Mg 0.2	9.946	1.92
Brain	H 10.7; C 14.5; N 2.2; O 71.2; Cl 0.3; Na 0.2; P 0.4; S 0.2; K 0.2	8.879	1.04
Water	H 66.6; O 33.3	10.020	1.00

The most important problem for radiotherapy is whether the desired dose can be delivered to the target point correctly. To this end, attempts were made to determine and calibrate the correct dose using the water phantom before radiation therapy [19]. Since the basic component of the human body is water, it is the most important material frequently used in the field of medical physics. Reliability of dose and LET calculations for the water target and accurate calculation of their distribution are reliable for patient treatments. In this regard, the structure, shape and design of the phantom to be used are important. In the literature, some phantom types used in treatment planning for different regions and organs of the human body in radiotherapy applications are described [22]. Plate and cylindrical phantoms are actively used to investigate dose or LET distribution and the factors affecting them [23]. For this reason, the phantom of the skull was used in the study (see its cross-section in Fig. 1). First, a phantom consisting only of water and brain tissues was used. Next, we took a cranial section of 0.6, 0.8 and 1.0 cm thick in the horizontal direction from left to right, and then a head half section containing enough water and brain tissue to reach a total thickness of 15 cm. Densities and basic compositions of tissues are given in Table 1. The TRIM simulation program determined these percentages according to the ICRU-276 report [24]. In the Geant4 simulation program, it was obtained from the Geant4 library (such as G4_WATER, G4_BRAIN_ICRP) [21].

Table 2

Bragg peaks for proton beams with different energies in the water phantom: comparison with RPTC experimental data [36]

Energy, MeV	TRIM (<i>a</i>)	GEANT (<i>b</i>)	RPTC (<i>c</i>)	Difference	
				(<i>a</i>) – (<i>c</i>)	(<i>b</i>) – (<i>c</i>)
90	6.21	5.65	5.50	0.71	0.15
100	7.26	6.98	6.83	0.43	0.15
110	9.00	8.70	8.28	0.72	0.42
120	10.50	10.18	9.80	0.70	0.38
130	12.00	11.65	11.45	0.55	0.20

Table 3

Calculation results for Bragg peak points produced by proton beams with different energies in the water phantom (using TRIM and GEANT4 simulation) and percentage differences

Energy, MeV	TRIM (<i>a</i>)	GEANT (<i>b</i>)	Difference, % (<i>a</i>) – (<i>b</i>)
60	2.82	2.42	14.18
70	3.91	3.41	12.79
80	5.01	4.52	9.78
90	6.21	5.65	9.02
100	7.26	6.98	3.86
110	9.00	8.70	3.33
120	10.5	10.18	3.05
130	12.00	11.65	2.92

In this study, cross-section phantom was used. The main motivation for using this phantom was to explore the effect of ionization of the proton beam when its passing through different layers of biomaterials. It is very difficult to process this research data in two different simulation systems using the same input directory. An account must be taken of the facts that TRIM only allows a single or multi-layer structured phantom, creates difficulties for 3D computation, and finally, such a computation will not make a significant contribution to achieving the goal of the study. For this reason, calculations were made only in 1D single and multi-layer structures.

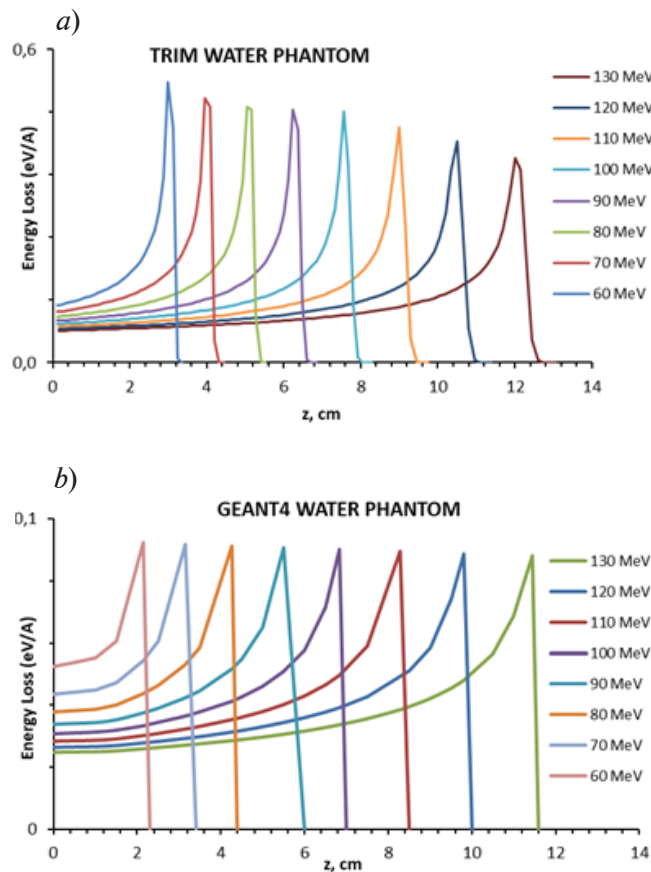


Fig. 2. Representation of Bragg curves for a 60 – 130 MeV proton beam in the water phantom from TRIM (a) and GEANT4 (b) simulation programs

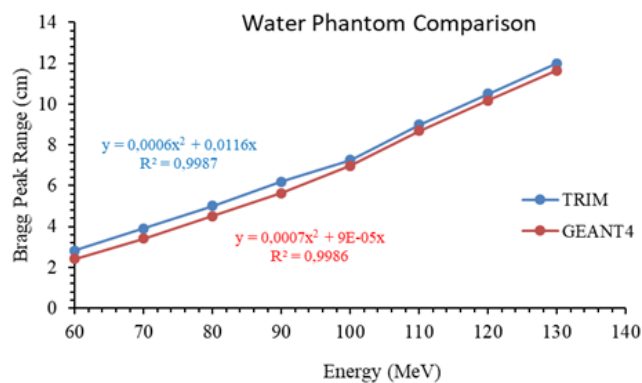


Fig. 3. Comparison of Bragg peaks for proton beams with different energies sent to the water phantom in two simulation systems

Table 4

Calculation results for Bragg peaks produced in the brain phantom by proton beams with different energies (TRIM and GEANT4 simulations were used) and percentage differences

Energy, MeV	TRIM (a)	GEANT (b)	Difference, % (a) – (b)
60	2.85	2.47	13.33
70	4.01	3.51	12.47
80	5.11	4.55	10.96
90	6.33	5.72	9.64
100	7.37	7.03	4.61
110	9.24	8.91	3.57
120	10.68	10.31	3.46
130	12.35	12.04	2.51

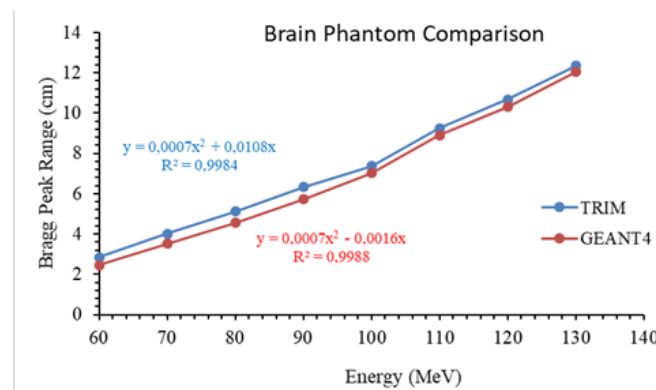


Fig. 4. Comparison of Bragg peaks produced in the brain phantom by proton beams with different energies (the two simulation codes were used)

Results

In this study, the effect of ionization interactions of protons passing through single or multiple layers on Bragg peak point was investigated for a cross-section phantom. The energy transferred per unit length of the proton beam to the layer or layers was taken into account. Therefore, the energy stored by the layer or layers per mass did not matter. In this connection, it was repeated in both simulation systems, taking into account the LET calculation. The Bragg peak positions (normalized to the maximum dose) for the water phantom irradiated by proton beams with different energies, in comparison with the experimental dose measurements of the Germany Rinecker Proton Therapy Center (RPTC) [27] are presented in Table 2. An average difference of 0.62 cm between RPTC and TRIM and that of 0.26 cm between RPTC and GEANT4 was found in the 90–130 MeV energy range.

Bragg peak points produced by the proton beams in the water phantom and obtained using TRIM and GEANT4 simulations are given in Table 3 and Figs. 2 and 3. As the energy of the proton beam increased, the difference between the Bragg peaks measured in the two simulation systems approached the difference ($\leq 5\%$) acceptable in medical physics. An average difference of 7.37% difference was found for all proton beam energies between the two simulation systems.

The largest difference was observed for the proton beam of 60 MeV and the smallest one was for the proton beam of 130 MeV. It was established that there was an average difference of 0.4 cm between the two simulation systems. This result is considered to be reasonable and acceptable.

Table 4 and Fig. 4 present Bragg peak points produced by the proton beams in the brain



Table 5

Calculation results for Bragg peaks produced in the *water phantom* with different cortical bone thicknesses by proton beams (the two simulation systems were used) and their differences

W , MeV	Cortical bone thickness for water phantom						Difference		
	0.6 cm		0.8 cm		1.0 cm		(a)–(b)	(c)–(d)	(e)–(f)
	TRIM (a)	GEANT4 (b)	TRIM (c)	GEANT4 (d)	TRIM (e)	GEANT4 (f)			
60	2.65	2.28	2.53	2.19	2.38	2.06	<u>0.37</u> 13.96%	<u>0.34</u> 13.44%	<u>0.32</u> 13.45%
70	3.59	3.12	3.48	3.04	3.36	2.93	<u>0.47</u> 13.09%	<u>0.44</u> 12.64%	<u>0.43</u> 12.80%
80	4.68	4.21	4.58	4.09	4.48	3.97	<u>0.47</u> 10.04%	<u>0.49</u> 10.70%	<u>0.51</u> 11.38%
90	5.93	5.34	5.85	5.26	5.58	5.02	<u>0.59</u> 9.95%	<u>0.59</u> 10.09%	<u>0.56</u> 10.04%
100	7.18	6.53	7.11	6.41	6.88	6.24	<u>0.65</u> 9.05%	<u>0.70</u> 9.85%	<u>0.64</u> 9.30%
110	8.58	8.24	8.53	8.18	8.32	8.02	<u>0.34</u> 3.96%	<u>0.35</u> 4.10%	<u>0.30</u> 3.61%
120	10.14	9.85	9.95	9.65	9.79	9.48	<u>0.29</u> 2.86%	<u>0.30</u> 3.02%	<u>0.31</u> 3.17%
130	11.71	11.51	11.53	11.45	11.36	11.28	<u>0.20</u> 1.71%	<u>0.08</u> 0.69%	<u>0.08</u> 0.70%

Notation: W is the proton beam energy.

phantom. These results were obtained in accordance with the parameters given in Table 1 and by using the TRIM and GEANT4 simulations.

As the energy of the proton beam increased, the difference between the Bragg peaks measured in the two simulation systems approached the difference ($\leq 5\%$) acceptable in medical physics. An average difference of 7.57% was found between the two simulation codes for all proton beam energies. The largest difference occurred in the proton beam of 60 MeV and the smallest one did in the proton beam of 130 MeV. An average difference of 0.43 cm between the two simulation systems was obtained. These results are considered to be reasonable and acceptable.

In the phantom geometry of the head section (see Fig. 1), the section I is water; the cranium 2 was selected in three different thicknesses: of 0.6, 0.8 and 1.0 cm. Using TRIM and GEANT4 simulations, the Bragg peak points produced by the proton beams in the phantom were calculated (Table 5).

An analysis of the obtained results makes possible to conclude that the difference between the two simulation programs decreased as the energy of the proton beam increased in all three cranium thicknesses. The Bragg peak difference between the two simulation codes was 8% on average for all three cranium thicknesses. The average Bragg peak difference between the two simulation codes was 0.42 cm at 0.6 cm cranium thickness, 0.41 cm at 0.8 cm cranium thickness and 0.39 cm at 1.0 cm cranium thickness. For 0.6 cm cranium thickness, an average difference of 0.28 cm was found in TRIM between the Bragg peaks (see Tables 4 and 5), while a difference of 0.30 cm was found in GEANT4. Similarly, an average difference of 0.39 cm in TRIM and of 0.41 cm in GEANT4 were found for 0.8 cm cranium thickness, 0.57 cm in TRIM and 0.56 cm in GEANT4 for 1.0 cm cranium thickness. The differences found in the two simulation codes were considered to be at an acceptable level.

In the phantom cross-section (see Fig. 1 again), the section (I) is the brain tissue and the cranium (2) was selected in three different thicknesses: of 0.6, 0.8 and 1.0 cm. The Bragg peaks produced by the proton beams in the brain phantom are given in Table 6 (TRIM and GEANT4 simulations

Table 6

Calculation results for Bragg peaks produced in the *brain phantom* with different cortical bone thicknesses by proton beams (the two simulation systems were used) and their differences

W , MeV	Cortical bone thickness for brain phantom						Difference		
	0.6 cm		0.8 cm		1.0 cm		(a)–(b)	(c)–(d)	(e)–(f)
	TRIM (a)	GEANT4 (b)	TRIM (c)	GEANT4 (d)	TRIM (e)	GEANT4 (f)			
60	2.65	2.26	2.52	2.18	2.40	2.08	$\frac{0.39}{14.72\%}$	$\frac{0.34}{13.49\%}$	$\frac{0.32}{13.33\%}$
70	3.58	3.10	3.48	3.05	3.32	2.95	$\frac{0.48}{13.41\%}$	$\frac{0.43}{12.36\%}$	$\frac{0.37}{11.15\%}$
80	4.68	4.22	4.57	4.07	4.46	3.98	$\frac{0.46}{9.83\%}$	$\frac{0.50}{10.94\%}$	$\frac{0.48}{10.76\%}$
90	5.92	5.35	5.84	5.26	5.49	5.04	$\frac{0.57}{9.63\%}$	$\frac{0.58}{9.93\%}$	$\frac{0.45}{8.20\%}$
100	7.17	6.54	7.12	6.41	6.86	6.25	$\frac{0.63}{8.79\%}$	$\frac{0.71}{9.97\%}$	$\frac{0.61}{8.89\%}$
110	8.56	8.25	8.51	8.19	8.29	8.05	$\frac{0.31}{3.62\%}$	$\frac{0.32}{3.76\%}$	$\frac{0.24}{2.90\%}$
120	10.12	9.84	9.94	9.66	9.76	9.49	$\frac{0.28}{2.77\%}$	$\frac{0.28}{2.82\%}$	$\frac{0.27}{2.77\%}$
130	11.69	11.53	11.52	11.44	11.32	11.27	$\frac{0.16}{1.37\%}$	$\frac{0.08}{0.69\%}$	$\frac{0.05}{0.44\%}$

Notation: W is the proton beam energy.

were used). Analyzing this data, it was seen that the difference between the two simulation programs decreased as the energy of the proton beam increased in all three cranium thicknesses. The average Bragg peak difference between the two simulation codes was 0.41 cm for 0.6 cm cranium thickness, 0.41 cm for 0.8 cm cranium thickness and 0.35 cm for 1.0 cm cranium thickness.

Discussion

In the presented study, the Bragg curves obtained by the virtual proton beams in the phantoms both homogeneous (the water) and heterogeneous (the brain) were confirmed by experimental data. The results obtained in the two simulation systems were found to be in agreement with the experimental data. It has been observed that the Bragg peak position formed by the proton beam in the energy range of 60 – 130 MeV is different from the water and brain phantom. This difference averages 0.15 cm for TRIM and 0.13 cm for GEANT4. Thus, it was seen in both simulation systems that the Bragg peak position formed by the proton beam was deeper in the brain phantom. The difference between the Bragg peak positions of the proton beam and TRIM and GEANT4 simulations; it was found to be 7.4 % in the water phantom and 7.6 % in the brain one. We believe that the difference arises from atomic collisions, since brain tissue contains different atoms. Further studies are needed to cover the entire range of beam energies, target thicknesses and target materials, mainly, for therapeutic applications in this area.

Experimental measurements are also required to compare Monte Carlo codes [28 – 32]. In a different study, where microdosimetric measurements of monoenergetic and modulated Bragg peaks of 62 MeV therapeutic proton beam were performed with a synthetic single crystal diamond microdosimeter, it was seen that the data of GEANT4 and TRIM [33] were comparable, as it was in our study. In another study with GEANT4 and TRIM, the ionizations of proton beams on different targets were examined, and it was seen that the results were close to each other similar to our results [34, 35].



In order to understand the behavior of the Bragg peak in cortical bone, being denser than the water and brain, the same calculations were repeated and compared using the selected TRIM and GEANT4 simulation programs. Thus, the Bragg peak positions formed in the water phantom (made with TRIM) and the cortical bony water phantom of three different thicknesses were compared. Average differences of 0.28 cm for 0.6 cm thickness, 0.39 cm for 0.8 cm thickness and 0.57 cm for 1.0 cm thickness were found. Comparing the Bragg peak positions in the water phantom simulated in GEANT4 by a similar method and in the water phantom of a cortical bone with three different thicknesses, we determined an average difference of 0.30 cm for 0.6 cm thickness, 0.41 cm for 0.8 cm thickness and 0.56 cm for 1.0 cm thickness.

Comparing TRIM and GEANT4 in water phantom and the cortical bony water phantom with three different thicknesses by the same method, we found an average difference of 0.42 cm for 0.6 cm thickness, an average difference of 0.41 cm for 0.8 cm thickness, and an average difference of 0.39 cm for 1.0 cm thickness. Then the brain phantom and the one with three different thicknesses of cortical bones were compared. The difference in 0.6 cm thickness was found to be 0.41 cm on average, the difference in 0.8 cm thickness was 0.41 cm on average, and the difference in 1.0 cm thickness was 0.35 cm on average. These differences were found to be 8.0 % on average. The calculations used in our studies include a probability due to the properties of the Monte-Carlo computing. Therefore, the calculations from the two simulation programs were consistent.

The effect of materials of different densities and thicknesses on the proton beam is important for proton therapy [36]. For this reason, the proton beam passing through the cooling materials of different thicknesses was investigated in Geant4 and TRIM MC simulation codes. The results of the available simulations were also compared with the calculation results based on the NIST PSTAR and CSDA models, and the differences were presented in the same way as in this publication [37]. In similar studies, particularly in the study of demonstrating this effect with different simulation systems, the results obtained by Geant4 were compared with those obtained by TRIM [36, 38]. The change exhibited by the proton beam in the presence of cortical bone of different thickness used for both phantoms was compared with previous data and showed a good agreement [5, 6, 14]. In addition, considering the advantages of the two simulation systems, the recoil interactions of the proton beams within the target were investigated. The obtained results were also compared in the same way as in this study [39]. The ion spacing was estimated using the TRIM code and was found to be compatible with that obtained by GEANT4 [40].

In the literature, some authors tried to find Bragg peak positions performing calculations of Bragg curves given by proton beams with 100, 120 and 130 MeV energies while their passing through the water phantoms, using different MC-based simulation programs (FLUKA, GATE, MCNPX, PTRAN and PHITS). Then they tried to compare the results obtained (similar to the procedure taken in our study). Bragg peak positions obtained in the literature were compared with the values determined in this study. In this comparison, an average difference of 4.1 % in TRIM and 7.5 % in GEANT4 was found for a proton beam with 100 MeV energy [41–46]. An average difference of 1.4 % in TRIM and 1.7 % in GEANT4 was found in the 120 MeV energy proton beam [41, 47]. An average difference of 6.7 % in TRIM and 3.9% in GEANT4 was found in the proton beam with 130 MeV energy [44]. It has been seen that this difference is due to the features of MC simulation, calculation parameters and statistical reasons such as probability.

Summary

Since there is no experimental heavy ion beam line, it was decided to use MC TRIM and GEANT4 simulation programs in this study. In keeping with the current approach, a water phantom was used to validate patient radiotherapy plans for heavy ion therapy. We report on MC TRIM and GEANT4 data on LET values of four new proton beams in water and brain phantoms with energies ranging from 60 to 130 MeV/u in increments of 10 MeV and in cortical bony water and brain phantoms of different thicknesses (0.6, 0.8 and 1.0 cm). These values were compared with hospital data and other studies in the literature. It has been suggested to be repeated in Teflon, titanium alloys ($\text{Ti}_6\text{Al}_4\text{V}$ and Nital) and Al_2O_3 ceramic alloys [15], which give the closest results to bone among the biomaterials used instead of cortical bone. In these studies, recoil effects, besides ionization, were considered and compared using the TRIM and GEANT4 simulation system.

REFERENCES

1. **Durante M., Loeffler J. S.**, Charged particles in radiation oncology. *Nature Rev. Clin. Oncol.* 7 (1) (2010) 37–43.
2. Particle therapy co-operative group (PTCOG). An organization for those uninterested in proton, light ion and heavy charged particle radiotherapy. URL: <https://www.ptcog.ch/>. Accessed: 2019-10-10.
3. **Kozłowska W. S., Böhlen T. T., Cuccagna C., et al.**, FLUKA particle therapy tool for Monte Carlo independent calculation of scanned proton and carbon ion beam therapy, *Phys. Med. Biol.* 64 (7) (2019) 075012.
4. **Schardt D., Elsässer T., Schulz-Ertner D.**, Heavy-ion tumor therapy: Physical and radiobiological benefits, *Rev. Mod. Phys.* 82 (1) (2010) 383–425.
5. **Senirkentli G. B., Ekinci F., Bostanci E., Güzel M. et al.**, Proton therapy for mandibula plate phantom, *Healthcare.* 9 (2) (2021) 167.
6. **Ekinci F., Bostanci E., Dağlı Ö., Güzel M. S.**, Analysis of Bragg curve parameters and lateral straggle for proton and carbon beam, *Commun. Fac. Sci. Univ. Ank., Ser. A2–A3.* 63 (1) (2021) 32–41.
7. **Chacon A., Safavi-Naevini M., Bolst D., et al.**, Monte Carlo investigation of the characteristics of radioactive beams for heavy ion therapy, *Sci. Rep.* 9 (1) (2019) 6537.
8. **Hong L., Goitein M., Bucciolini M., et al.**, A pencil beam algorithm for proton dose calculations, *Phys. Med. Biol.* 41 (8) (1996) 1305–1330.
9. **Rogers D. W. O.**, Fifty years of Monte Carlo simulations for medical physics, *Phys. Med. Biol.* 51 (13) (2016) R287–R301.
10. **Baiocco G., Barbieri S., Babini G., et al.**, The origin of neutron biological effectiveness as a function of energy, *Sci. Rep.* 6 (September) (2016) 34033.
11. **Kajimoto T., Tanaka K., Endo S., et al.**, Double differential cross sections of neutron production by 135 and 180 MeV protons on A-150 tissue-equivalent plastic, *Nucl. Instr. Meth. Phys. Res. B.* 487 (2021) 38–44.
12. **Kurosu K., Das I. J., Moskvin V. P.**, Optimization of GATE and PHITS Monte Carlo code parameters for spot scanning proton beam based on simulation with FLUKA general-purpose code, *Nucl. Instr. Meth. Phys. Res. B.* 367 (2016) 14–25.
13. **Lund C. M., Famulari G., Montgomery L., Kildea J.**, A microdosimetric analysis of the interactions of mono energetic neutrons with human tissue, *Physica Medica.* 73 (May) (2020) 29–42.
14. **Ekinci F., Bölükdemir M. H.**, The effect of the second peak formed in biomaterials used in a slab head phantom on the proton Bragg peak, *J. Polytech.* 23 (1) (2019) 129–136.
15. **Augusto R. S., Bauer J., Bouhali O., et al.**, An overview of recent developments in FLUKA PET TOOLS, *Physica Medica.* 54 (October) (2018) 189–199.
16. **Titt U., Bednarz B., Paganetti H.**, Comparison of MCNPX and Geant4 proton energy deposition predictions for clinical use, *Phys. Med. Biol.* 57 (20) (2012) 6381–6393.
17. **Wu J.-C., Feng Q.-J., Liu X.-K., et al.**, A combination method for simulation of secondary knock-on atoms of boron carbide induced by neutron irradiation in SPRR-300, *Nucl. Instr. Meth. Phys. Res. B.* 368 (1 February) (2016) 1–4.
18. **Ogilvy C. S., Stieg Ph. E., Awad I., et al.**, Recommendations for the management of intracranial arteriovenous malformations, *Stroke.* 32 (6) (2001) 1458–1471.
19. **Shaller C., Schramm J., Huan D.**, Significance of factors contributing to surgical complications and to late outcome after elective surgery of cerebral arteriovenous malformations, *J. Neurol. Neurosurg. Psychiat.* 65 (4) (1998) 547–554.
20. **Ogilvy C. S.**, Radiation therapy for arteriovenous malformations: a review, *Neurosurg.* 26 (5) (1990) 725–735.
21. Geant4. URL: <http://www.geant4.org/geant4/>, Son Erişim Tarihi: 20.04.2016.
22. **Jafar J. J., Davis A. J., Berenstein A., et al.**, The effect of embolization with N-butyl cyanoacrylate prior to surgical resection of cerebral arteriovenous malformations, *J. Neurosurg.* 78 (1) (1993) 60–69.
23. **Behrens R., Hupe O.**, Influence of the phantom shape (slab, cylinder or Alderson) on the performance of an Hp(3) eye dosimeter, *Rad. Protect. Dosim.* 168 (4) (2015) 441–449.
24. **Van Rooij W. J., Sluzewski M., Beute G. N.**, Brain AVM embolization with Onyx, *Am. J. Neurorad.* 28 (1) (2007) 172–178.
25. **Ziegler J. F.** SRIM – The stopping and range of ion in matter (2007). URL: <https://www.srim.org/> Accessed: 20.09.2019.



26. ICRU-1992: Photon, electron, proton and neutron interaction data for body tissues, Report 46 of The International Commission on Radiation Units and Measurements (ICRU), National Bureau of Standards, USA: US Department of Commerce, 1992.
27. Rinecker Proton Therapy Center (RPTC), Munich, Germany. URL: <https://www.rptc.de/en/home.html>. Son Ulaşım: 20 Aralık 2017.
28. **Battistoni G., Cerutti F., Fassò A., et al.**, The FLUKA code: description and benchmarking, AIP Conf. Proc. 896 (2007) 31–49.
29. **Mairani A.**, Nucleus-nucleus interaction modelling and applications in ion therapy treatment planning, PhD Thesis, Univesity of Pavia, Italy (2017).
30. **Böhlen T. T., Cerutti F., Chin M. P. W., et al.**, The FLUKA code: Developments and challenges for high energy and medical applications, Nucl. Data Sheets. 120 (June) (2014) 211–214.
31. **Dudouet J., Cussol D., Durand D., Labalme M.**, Benchmarking GEANT4 nuclear models for hadron therapy with 95 MeV/nucleon carbon ions, Phys. Rev. C. 89 (5) (2014) 054616.
32. **Aricò G., Gehrke T., Gallas R., et al.**, Investigation of single carbon ion fragmentation in water and PMMA for hadron therapy, Phys. Med. Biol. 64 (5) (2019) 055018.
33. **Verona C., Cirrone G. A. P., Magrin G., et al.**, Microdosimetric measurements of a monoenergetic and modulated Bragg peaks of 62 MeV therapeutic proton beam with a synthetic single crystal diamond microdosimeter, Med. Phys. 47 (11) (2020) 5791–5801.
34. **Wu Z., Chen S.**, Heavy ion, proton and neutron charge deposition analyses in several semiconductor materials, IEEE Trans. Nucl. Sci. 65 (8) (2018) 1791–1799.
35. **Du Q., Lin S. T., He H. T., et al.**, Response of gadolinium doped liquid scintillator to charged particles: measurement based on intrinsic U/Th contamination, J. Instrum. 13 (4) (2018) P04001.
36. **Mastromarco M., Digennaro A., Mazzone A., et al.**, Proton boron capture therapy: Dose calculations and a possible new measurement, RAD Conf. Proc. 4 (2020) 185–189.
37. **Yevseyeva O., de Assis J., Yevseev I., et al.**, Comparison of GEANT4 simulations with experimental data for thick Al absorbers, AIP Conf. Proc. 1139 (2009) 97–101.
38. **Liu T. Q., Lic D. Q., Caic C., et al.**, Heavy ion track straggling effect in single event effect numerical simulation of 3D stacked devices, Microelectr. Rel. 114 (November) (2020) 113853.
39. **Zheng Y., Zheng J., Wang X.**, Study on the applicability of neutron radiation damage method used for high-temperature superconducting tape based on Geant4 and SRIM, Sci. Technol. Nucl. Instal. (24 November) (2021) ID 2839746.
40. **Parida M. K., Prabakar K., Prasanna G., Sundari S. T.**, Efficiency of boric acid coated semiconductor neutron detector – A GEANT4 simulation study, In: Proc. The 14th IEEE India Council International Conference (INDICON), 2017. doi:10.1109/indicon.2017.8487978.
41. **Schwarz M.**, Treatment planning in proton therapy, Europ. Phys. J. Plus. 126 (7) (2011) 67.
42. **Jia X., Schümann, J., Paganetti, H., ve Jiang S. B.**, GPU-based fast Monte Carlo dose calculation for proton therapy, Phys. Med. Biol. 57 (23) (2012) 7783.
43. **Yang Z. Y., Tsai P. E., Lee S. C., et al.**, Inter-comparison of dose distributions calculated by FLUKA, GEANT4, MCNP, and PHITS for proton therapy, Europ. Phys. J., Web of Conf. 153 (2017) 04011.
44. **Jia S. B., Hadizadeh M. H., Mowlavi A. A., ve Loushab M. E.**, Evaluation of energy deposition and secondary particle production in proton therapy of brain using a slab head phantom, Rep. Pract. Oncol. Radiother. 19 (6) (2014) 376–384.
45. **Sterpin E., Sorriaux J., Vynckier S.**, Extension of PENELOPE to protons: Simulation of nuclear reactions and benchmark with Geant4, Med. Phys. 40 (11) (2013) 111705.
46. **Grimes D. R., Warren D. R., Partridge M.**, An approximate analytical solution of the Bethe equation for charged particles in the radiotherapeutic energy range, Sci. Rep. 7 (1) (2017) 9781.
47. **Almhagen E.**, Development and validation of a scanned proton beam model for dose distribution verification using Monte Carlo, Thesis for Master of Science in Medical Radiation Physics. (2015) 48–49.

СПИСОК ЛИТЕРАТУРЫ

1. **Durante M., Loeffler J. S.** Charged particles in radiation oncology // *Nature Reviews Clinical Oncology*. 2010. Vol. 7. No. 1. Pp. 37–43.
2. Particle therapy co-operative group (PTCOG). An organization for those interested in proton, light ion and heavy charged particle radiotherapy. URL: <https://www.ptcog.ch/>. Accessed: 2019-10-10.
3. **Kozłowska W. S., Böhlen T. T., Cuccagna C., Ferrari A., Fracchiolla F., Magro G., Mairani A., Schwarz M., Vlachoudis V., Georg D.** LUKA particle therapy tool for Monte Carlo independent calculation of scanned proton and carbon ion beam therapy // *Physics in Medicine & Biology*. 2019. Vol. 64. No. 7. P. 075012.
4. **Schardt D., Elsässer T., Schulz-Ertner D.** Heavy-ion tumor therapy: Physical and radiobiological benefits // *Review of the Modern Physics*. 2010. Vol. 82. No. 1. Pp. 383–425.
5. **Senirkentli G. B., Ekinci F., Bostanci E., Güzel M. S., Dağlı Ö., Karim A. M., Mishra A.** Proton therapy for mandibula plate phantom // *Healthcare*. 2021. Vol. 9. No. 2. P. 167.
6. **Ekinci F., Bostanci E., Dağlı Ö., Güzel M. S.** Analysis of Bragg curve parameters and lateral straggle for proton and carbon beam // *Communications Faculty of Sciences University of Ankara. Ser. A2–A3*. 2021. Vol. 63. No. 1. Pp. 32–41.
7. **Chacon A., Safavi-Naevini M., Bolst D., et al.** Monte Carlo investigation of the characteristics of radioactive beams for heavy ion therapy // *Scientific Reports*. 2019. Vol. 9. No. 1. P. 6537.
8. **Hong L., Goitein M., Bucciolini M., Comiskey R., Gottschalk B., Rosenthal S., Serago C., Urie M.** A pencil beam algorithm for proton dose calculations // *Physics in Medicine & Biology*. 1996. Vol. 41. No. 8. Pp. 1305–1330.
9. **Rogers D. W. O.** Fifty years of Monte Carlo simulations for medical physics // *Physics in Medicine & Biology*. 2006. Vol. 51. No. 13. Pp. R287–R301.
10. **Baiocco G., Barbieri S., Babini G., et al.** The origin of neutron biological effectiveness as a function of energy // *Scientific Reports*. 2016. Vol. 6. September. P. 34033.
11. **Kajimoto T., Tanaka K., Endo S., Kamada S., Tanaka H., Takada M., Hamano T.** Double differential cross sections of neutron production by 135 and 180 MeV protons on A-150 tissue-equivalent plastic // *Nuclear Instruments and Methods in Physics Research B: Beam Interactions with Materials and Atoms*. 2021. Vol. 487. Pp. 38–44.
12. **Kurosu K., Das I. J., Moskvina V. P.** Optimization of GATE and PHITS Monte Carlo code parameters for spot scanning proton beam based on simulation with FLUKA general-purpose code // *Nuclear Instruments and Methods in Physics Research B*. 2016. Vol. 367. Pp. 14–25.
13. **Lund C. M., Famulari G., Montgomery L., Kildea J.** A microdosimetric analysis of the interactions of mono energetic neutrons with human tissue // *Physica Medica*. 2020. Vol. 73. May. Pp. 29–42.
14. **Ekinci F., Bölükdemir M. H.** The effect of the second peak formed in biomaterials used in a slab head phantom on the proton Bragg peak // *Journal of Polytechnic*. 2019. Vol. 23. No. 1. Pp. 129–136.
15. **Augusto R. S., Bauer J., Bouhali O., et al.** An overview of recent developments in FLUKA PET TOOLS // *Physica Medica*. 2018. Vol. 54. October. Pp. 189–199.
16. **Titt U., Bednarz B., Paganetti H.** Comparison of MCNPX and Geant4 proton energy deposition predictions for clinical use // *Physics in Medicine and Biology*. 2012. Vol. 57. No. 20. Pp. 6381–6393.
17. **Wu J.-C., Feng Q.-J., Liu X.-K., Zhan C.-Y., Zou Y., Liu Y.-G.** A combination method for simulation of secondary knock-on atoms of boron carbide induced by neutron irradiation in SPRR-300 // *Nuclear Instruments and Methods in Physics Research B*. 2016. Vol. 368. 1 February. Pp. 1–4.
18. **Ogilvy C. S., Stieg Ph. E., Awad I., et al.** Recommendations for the management of intracranial arteriovenous malformations // *Stroke*. 2001. Vol. 32. No. 6. Pp. 1458–1471.
19. **Shaller C., Schramm J., Huan D.** Significance of factors contributing to surgical complications and to late outcome after elective surgery of cerebral arteriovenous malformations // *Journal of Neurology, Neurosurgery & Psychiatry*. 1998. Vol. 65. No. 4. Pp. 547–554.
20. **Ogilvy C. S.** Radiation therapy for arteriovenous malformations: a review, *Neurosurg.* 26 (5) (1990) 725–735.
21. Geant4. URL: <http://www.geant4.org/geant4/>, Son Erişim Tarihi: 20.04.2016.
22. **Jafar J. J., Davis A. J., Berenstein A., et al.** The effect of embolization with N-butyl cyanoacrylate prior to surgical resection of cerebral arteriovenous malformations, *J. Neurosurg.* 78 (1) (1993) 60–69.
23. **Behrens R., Hupe O.** Influence of the phantom shape (slab, cylinder or Alderson) on the performance of an Hp(3) eye dosimeter, *Rad. Protect. Dosim.* 168 (4) (2015) 441–449.



24. **Van Rooij W. J., Sluzewski M., Beute G. N.,** Brain AVM embolization with Onyx, *Am. J. Neurorad.* 28 (1) (2007) 172–178.
25. **Ziegler J. F.** SRIM – The stopping and range of ion in matter (2007). URL: <https://www.srim.org/> Accessed: 20.09.2019.
26. ICRU-1992: Photon, electron, proton and neutron interaction data for body tissues, Report 46 of The International Commission on Radiation Units and Measurements (ICRU), National Bureau of Standards, USA: US Department of Commerce, 1992.
27. Rinecker Proton Therapy Center (RPTC), Munich, Germany. URL: <https://www.rptc.de/en/home.html>. Son Ulaşım: 20 Aralık 2017.
28. **Battistoni G., Cerutti F., Fassò A., et al.,** The FLUKA code: description and benchmarking, *AIP Conf. Proc.* 896 (2007) 31–49.
29. **Mairani A.,** Nucleus-nucleus interaction modelling and applications in ion therapy treatment planning, PhD Thesis, University of Pavia, Italy (2017).
30. **Böhlen T. T., Cerutti F., Chin M. P. W., et al.,** The FLUKA code: Developments and challenges for high energy and medical applications, *Nucl. Data Sheets.* 120 (June) (2014) 211–214.
31. **Dudouet J., Cussol D., Durand D., Labalme M.,** Benchmarking GEANT4 nuclear models for hadron therapy with 95 MeV/nucleon carbon ions, *Phys. Rev. C.* 89 (5) (2014) 054616.
32. **Aricò G., Gehrke T., Gallas R., et al.,** Investigation of single carbon ion fragmentation in water and PMMA for hadron therapy, *Phys. Med. Biol.* 64 (5) (2019) 055018.
33. **Verona C., Cirrone G. A. P., Magrin G., et al.,** Microdosimetric measurements of a monoenergetic and modulated Bragg peaks of 62 MeV therapeutic proton beam with a synthetic single crystal diamond microdosimeter, *Med. Phys.* 47 (11) (2020) 5791–5801.
34. **Wu Z., Chen S.,** Heavy ion, proton and neutron charge deposition analyses in several semiconductor materials, *IEEE Trans. Nucl. Sci.* 65 (8) (2018) 1791–1799.
35. **Du Q., Lin S. T., He H. T., et al.,** Response of gadolinium doped liquid scintillator to charged particles: measurement based on intrinsic U/Th contamination, *J. Instrum.* 13 (4) (2018) P04001.
36. **Mastromarco M., Digennaro A., Mazzone A., et al.,** Proton boron capture therapy: Dose calculations and a possible new measurement, *RAD Conf. Proc.* 4 (2020) 185–189.
37. **Yevseyeva O., de Assis J., Yevseev I., et al.,** Comparison of GEANT4 simulations with experimental data for thick Al absorbers, *AIP Conf. Proc.* 1139 (2009) 97–101.
38. **Liu T. Q., Lic D. Q., Caic C., et al.,** Heavy ion track straggling effect in single event effect numerical simulation of 3D stacked devices, *Microelectr. Rel.* 114 (November) (2020) 113853.
39. **Zheng Y., Zheng J., Wang X.,** Study on the applicability of neutron radiation damage method used for high-temperature superconducting tape based on Geant4 and SRIM, *Sci. Technol. Nucl. Instal.* (24 November) (2021) ID 2839746.
40. **Parida M. K., Prabakar K., Prasanna G., Sundari S. T.,** Efficiency of boric acid coated semiconductor neutron detector – A GEANT4 simulation study, In: *Proc. The 14th IEEE India Council International Conference (INDICON), 2017.* doi:10.1109/indicon.2017.8487978.
41. **Schwarz M.,** Treatment planning in proton therapy, *Europ. Phys. J. Plus.* 126 (7) (2011) 67.
42. **Jia X., Schümann, J., Paganetti, H., ve Jiang S. B.,** GPU-based fast Monte Carlo dose calculation for proton therapy, *Phys. Med. Biol.* 57 (23) (2012) 7783.
43. **Yang Z. Y., Tsai P. E., Lee S. C., et al.,** Inter-comparison of dose distributions calculated by FLUKA, GEANT4, MCNP, and PHITS for proton therapy, *Europ. Phys. J., Web of Conf.* 153 (2017) 04011.
44. **Jia S. B., Hadizadeh M. H., Mowlavi A. A., ve Loushab M. E.,** Evaluation of energy deposition and secondary particle production in proton therapy of brain using a slab head phantom, *Rep. Pract. Oncol. Radiother.* 19 (6) (2014) 376–384.
45. **Sterpin E., Sorriaux J., Vynckier S.,** Extension of PENELOPE to protons: Simulation of nuclear reactions and benchmark with Geant4, *Med. Phys.* 40 (11) (2013) 111705.
46. **Grimes D. R., Warren D. R., Partridge M.,** An approximate analytical solution of the Bethe equation for charged particles in the radiotherapeutic energy range, *Sci. Rep.* 7 (1) (2017) 9781.
47. **Almhagen E.,** Development and validation of a scanned proton beam model for dose distribution verification using Monte Carlo, Thesis for Master of Science in Medical Radiation Physics. (2015) 48–49.

THE AUTHORS

EKINCI Fatih

Gazi University, Physics Department, Besevler, Ankara, Turkey
Emniyet Mahallesi Bandırma Caddesi No: 6/9 06500 Yenimahalle/ANKARA
fatih.ekinci2@gazi.edu.tr
ORCID: 0000-0002-1011-1105

BOSTANCI Erkan

Ankara University, Computer Engineering Department, Golbasi, Ankara, Turkey
ebostanci@ankara.edu.tr
ORCID: 0000-0001-8547-7569

GÜZEL Mehmet Serdar

Ankara University, Computer Engineering Department, Golbasi, Ankara, Turkey
mguzel@ankara.edu.tr
ORCID: 0000-0002-3408-0083

DAĞLI Özlem

Gazi University, Faculty of Medicine, Department of Neurosurgery Gamma Knife Unit, Ankara, Turkey
ozlemdagli@gazi.edu.tr
ORCID: 0000-0003-3798-8342

СВЕДЕНИЯ ОБ АВТОРАХ

ЭКИНДЖИ Фатих – доктор наук, профессор кафедры физики, факультета коммуникаций
Университета Гази, Бешевлер, г. Анкара, Турция.
Emniyet Mahallesi Bandırma Caddesi No: 6/9 06500 Yenimahalle/ANKARA
fatih.ekinci2@gazi.edu.tr
ORCID: 0000-0002-1011-1105

БОСТАНДЖИ Гази Эркан – кандидат наук, доцент кафедры вычислительной техники
Университета Анкары, Гельбаши, г. Анкара, Турция.
ebostanci@ankara.edu.tr
ORCID: 0000-0001-8547-7569

ГУЗЕЛЬ Мехмет Сердар – кандидат наук, доцент кафедры вычислительной техники
Университета Анкары, Гельбаши, г. Анкара, Турция.
mguzel@ankara.edu.tr
ORCID: 0000-0002-3408-0083

ДАГЛИ Озлем – сотрудница кафедры стереотоксической радиохирургии головного мозга
медицинского факультета Университета Гази, г. Анкара, Турция.
ozlemdagli@gazi.edu.tr
ORCID: 0000-0003-3798-8342

Received 01.03.2022. Approved after reviewing 25.04.2022. Accepted 25.04.2022.
Статья поступила в редакцию 01.03.2022. Одобрена после рецензирования 25.04.2022.
Принята 25.04.2022.